Accepted Manuscript
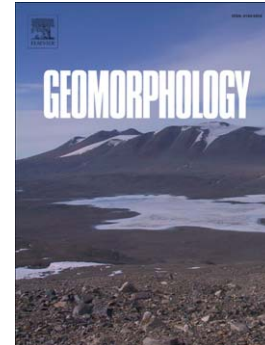
Flow deflection over a foredune

Patrick A. Hesp, Thomas A.G. Smyth, Peter Nielsen, Ian J. Walker, Bernard O. Bauer, Robin Davidson-Arnott

Please cite this article as: Hesp, Patrick A., Smyth, Thomas A.G., Nielsen, Peter, Walker, Ian J., Bauer, Bernard O., Davidson-Arnott, Robin, Flow deflection over a foredune, *Geomorphology* (2014), doi: 10.1016/j.geomorph.2014.11.005

Flow deflection over a foredune

Patrick A. Hesp[1], Thomas A.G. Smyth[1], Peter Nielsen[2], Ian J. Walker[3,] Bernard O. Bauer[4], and Robin Davidson-Arnott[5]

[1]School of the Environment, Faculty of Science and Engineering, Flinders University, Bedford Park, South Australia 5042

Patrick.hesp@flinders.edu.au; Thomas.smyth@flinders.edu.au

[2]School of Civil Engineering, University of Queensland, St Lucia, Qld. 4072

p.nielsen@uq.edu.au

[3]Dept of Geography, University of Victoria, P.O. Box 3060, Station CSC, Victoria, BC Canada V8W 3R4

ijwalker@uvic.ca

[4]Earth and Environmental Sciences & Geography, University of British Columbia, Okanagan, Kelowna, BC Canada V1V 1V7

bernard.bauer@ubc.ca

[5]Dept of Geography, University of Guelph, Guelph, ON Canada N1G2W1

rdarnott@uoguelph.ca

Flow deflection of surface winds is common across coastal foredunes and blowouts. Incident winds approaching obliquely to the dune toe and crestline tend to be deflected towards a more crest-normal orientation across the stoss slope of the foredune. This paper examines

field measurements for obliquely incident winds, and compares them to computational fluid dynamics (CFD) modelling of flow deflection in 10° increments from onshore (0°) to alongshore (90°) wind approach angles. The mechanics of flow deflection are discussed, followed by a comparative analysis of measured and modelled flow deflection data that shows strong agreement. CFD modelling of the full range of onshore to alongshore incident winds reveals that deflection of the incident wind flow is minimal at $0°$ and gradually increases as the incident wind turns towards $30°$ to the dune crest. The greatest deflection occurs between $30°$ and $70°$ incident to the dune crest. The degree of flow deflection depends secondarily on height above the dune surface, with the greatest effect near the surface and toward the dune crest. Topographically forced flow acceleration ("speed-up") across the stoss slope of the foredune is greatest for winds less than $30°$ (i.e., roughly perpendicular) and declines significantly for winds with more oblique approach angles. There is less lateral uniformity in the wind field when the incident wind approaches from $>60°$ because the effect of aspect ratio on topographic forcing and streamline convergence is less pronounced.

KEY WORDS: Foredune, flow deflection, Computational fluid dynamics (CFD), oblique winds.

Introduction

Flow deflection of near surface (i.e., z <10 m) winds approaching dunes and blowouts from an oblique angle is commonly observed (e.g., Svasek and Terwindt, 1974; Mikkelsen, 1989; Rasmussen, 1989; Arens et al., 1995; Hesp and Pringle, 2001; Hesp, 2002; Walker et al., 2006; 2009; Lynch et al., 2008, 2009, 2013; Smyth et al., 2011; 2012; 2013; 2014). Over coastal foredunes and other ridges such as transverse dunes, oblique winds tend to be deflected towards more crest-normal as the flow approaches and crosses the stoss slope of the

1

dune or ridge (e.g., Svasek and Terwindt, 1974; P. Jackson, 1977; 1979; Tsoar, 1983a, b; Walker et al., 2006; 2009; Lynch et al., 2008; 2010; Jackson et al., 2011; Bauer et al., 2012; Rubin and Rubin, 2013; Walker and Shugar, 2013). This phenomenon is important for several reasons, including: (i) oblique winds can transport sediment onto a foredune or away from it depending on the incidence angle (Arens, 1996; Walker et al., 2006; Lynch et al., 2008; 2010), thereby affecting the sediment supply to the dune system (Arens et al., 1995; Arens, 1996); (ii) wind deflection can strongly influence net transport pathways and sedimentation patterns on a foredune (Svasek and Terwindt, 1974; Hesp, 2002; Walker et al., 2006; 2009; Bauer et al., 2012); (iii) beach transport conditions may be decoupled from foredune transport conditions at certain approach angles (Bauer et al., 2012); (iv) sedimentary strata may be deposited more crest transverse than the wind regime would indicate (Hesp, 1988), thereby leading to erroneous paleo-environmental interpretations; and (v) fetch distances and sand transport pathways into and over dunes may be greater or less than predicted depending on the nature and magnitude of flow deflection (Svasek and Terwindt, 1974; Walker et al., 2006; 2009; Walker and Shugar, 2013).

Several studies have suggested that near-surface flow deflection occurs in response to pressure differences upwind of the dune toe and up the stoss slope (Svasek and Terwindt, 1974; Bradley, 1983; Mikkelsen, 1989). The resulting pressure gradient produces deviations of streamline orientations from the incident direction as a consequence of mass and momentum conservation. Reviews of related topographic forcing and steering effects in near-surface airflow over foredunes are provided in Walker et al. (2006; 2009), and over transverse ridges more generally (Finnigan et al., 1990; Weng et al., 1991; Wiggs et al., 1996; Belcher and Hunt, 1998, Wood, 2000; Parson et al., 2004; Ayotte and Hughes, 2004; Bauer et al., 2013; Walker and Shugar, 2013). The greatest deflection occurs when incident winds approach the dune at moderate to highly oblique approach angles (Mikkelsen, 1989).

According to Svasek and Terwindt (1974), maximum deflection occurs at incident angles between 30° and 60° and the degree of deflection is most pronounced near the surface (Mikkelsen, 1989; Walker et al., 2009). Bradley (1983) and Walker et al. (2009) found an inverse relationship between incident flow direction and speed, such that when the flow was more oblique to the dune crestline, the flow speed decreased over the dune (cf. Arens, 1995; 1996; Lynch et al., 2010; Jackson et al., 2011), which implies that less sand can be delivered to the foredune crest and lee-side region. Arens et al. (1995) found that, as winds became more oblique, the effective slope (i.e., aspect ratio) diminished and, in response, transport rates up the stoss slope decreased because topographically-forced flow acceleration is not as pronounced as with perpendicular approach angles.

The degree of flow steering found in empirical studies varies. Bradley (1983) examined flow over a long low hill in the field and found only slight deflection (~1-2°) of the obliquely incident winds. This may be a partly methodological issue because they compared winds at the crest to those at the base of the slope (rather than the incident conditions some distance upwind of the toe). Moreover, the topographic profile of the ridge was low. Walker et al. (2006; 2009) and Bauer et al. (2012) report that incident flow is already partly deflected at the base of a foredune. For a separate theoretical case, Bradley (1983) found a deflection of ~4° for an incident oblique wind approaching the ridge at 24°. Rasmussen (1989), following on the fieldwork of Mikkelsen (1989), examined flow vectors and steering at 1 m height over a 2-D symmetrical dune ridge. For an incident oblique wind 30° to crest-normal, Rasmussen (1989) found that flow was deflected more crest-normal by 10° by the mid-stoss slope and 15° by the dune crest. For flow approaching a steep, 70- to 90-m high scarp at an angle of 45° to normal, it was found that flow separated in front of the scarp base and was deflected alongshore, while higher up the scarp the flow crossed at an oblique angle. Arens et al. (1995) argued that flow deflection increased with increasing foredune height. They found

flow deflections of less than $15°$ up to $30°$ for low (1-2 m high) to high (12-15 m) foredunes, respectively.

Walker et al. (2006) examined flow responses over a foredune at Prince Edward Island (PEI), Canada, and found that the flow veered $7°$ from the backshore into the dune toe and another $12°$ from the dune toe to lower stoss slope, despite the regional flow being oblique offshore. At the same study site, Walker et al. (2009) found that, during very oblique incident flow conditions, there was significant deflection of flow (as much as $37°$) from the backshore to the crest of the 12-m high foredune. In a subsequent study at the PEI site, Bauer et al. (2012) documented pronounced deflection of oblique incident winds over the foredune, and found that wind directions on the beach during a storm event were far less variable than those on the dune crest for the same incident winds. During alongshore incident flow conditions Lynch et al. (2009) found that wind near the dune crest was deflected more offshore compared to the flow along the beach and, for obliquely onshore winds, they found a deflection of $\sim 20°$ towards shore-normal.

Despite the number of studies that have documented deflection of near-surface winds and that have speculated on the implications for aeolian transport pathways (e.g., Walker and Nickling, 2002; Baddock et al., 2007; Walker and Shugar, 2013), and its importance in contributing to foredune evolution and form, there have been few detailed studies dedicated to the nature of flow deflection, and little modelling of the process. In this paper, we examine the nature of flow deflection over a foredune for a full range of onshore to alongshore incident winds (0° to $90°$) using empirical observations and computational fluid dynamics modelling (CFD).

STUDY SITE AND METHODS

Study Site

The study site was located on a foredune within the Greenwich Dunes unit of Prince Edward Island National Park on the north-east shore of Prince Edward Island (PEI), Canada (Fig. 1). The field experiments were part of a study on the airflow and sedimentary dynamics of this beach-dune complex (e.g. Davidson-Arnott et al., 2003, 2008, 2009, 2012; Walker et al., 2003, 2006, 2009; Hesp et al, 2005, 2009, 2013; Bauer et al., 2009, 2012; Delgado-Fernandez and Davidson-Arnott, 2009; Hesp and Walker, 2012; Chapman et al., 2012, 2013;Delgado-Fernandez et al., 2013; Ollerhead et al., 2013).
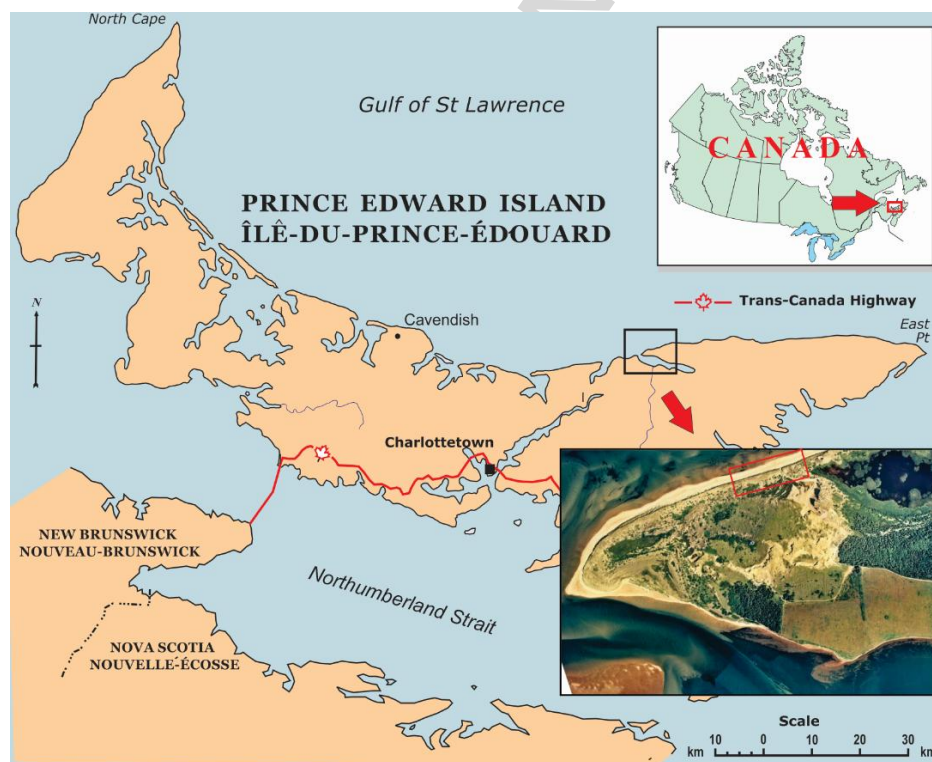

Figure 1: Location of the Greenwich dunes unit within Prince Edward Island National Park on P.E.I., Canada.

The foredune crest is ~10 m above mean water level with a steep stoss slope (20°-25°) and an ENE-WSW crestline orientation. The foredune has been stable in position and growing in

5

height since 1953 on this erosional coast (Ollerhead et al., 2013). The dune fronts onto a low-gradient, microtidal (~1 m), moderate to high energy intermediate beach with a low-tide width of about 35 m, and backs onto the deflation plain of a large parabolic dune (see Walker et al., 2009; Mathew et al., 2010). Two experiment lines were originally established on the foredune, one on a non-scarped section and one on an initially scarped section. The latter section is the line examined further in this study because this is where the high-frequency instrumentation was deployed. The foredune displayed a non-vegetated, 0.7-m high scarp at the initiation of experiments, which later filled in with sand following a significant wind storm (see Fig. 6 in Hesp et al., 2009). The dune is vegetated by *Ammophila breviligulata,* with plant heights averaging 0.3 m and with a spatial density ranging from 2 – 45% based on visual assessments on contiguous transects.
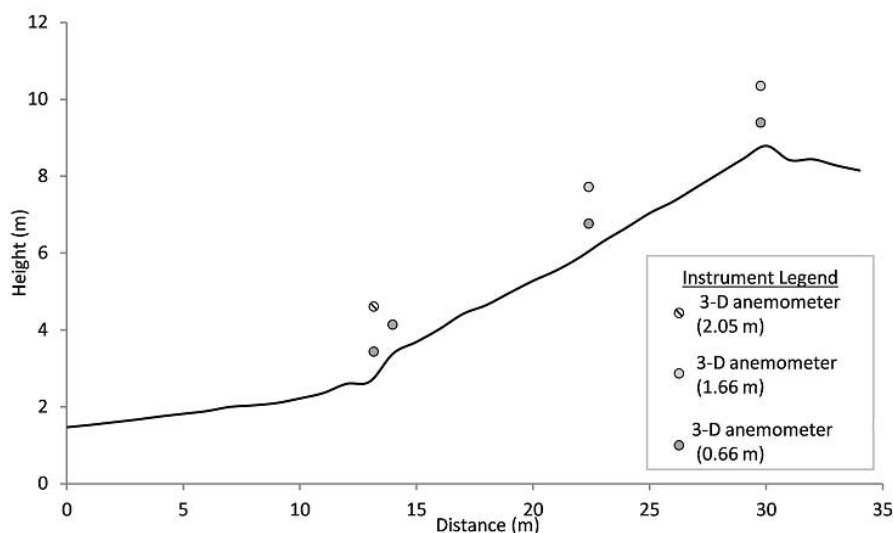
Experimental Methods and Set-up

Figure 2. Crest perpendicular profile of the foredune at Prince Edward Island. The locations of 3-D anemometers utilized in the field measurements are indicated by circles on the profile.

The data utilized for modelling comparison purposes were collected on the 11th October, 2004 during a moderate to gale force wind speed event (Tropical Storm Nicole - see Fig. 2 in

Hesp et al., 2009, Fig. 3 in Hesp et al., 2013, and Fig. 12 in Walker et al., 2009). In this investigation, wind speed was measured from 7 sonic anemometers on the dune stoss face and crest. A cup anemometer positioned at 4 m elevation and 12.34 m seawards of the dune toe on the beach provided incident wind conditions.

Three-dimensional velocity fields were measured with RM Young 3-D sonic anemometers aligned parallel to the slope (Fig. 2). These instruments have a wind speed resolution of 0.01 ms^{-1}, an accuracy of +/- 1% up to 30 ms^{-1}, and a wind direction resolution of 0.1° and an accuracy of +/- 2° up to 30 ms^{-1}. Pairs of sensors were deployed at 0.66 m, and 2.05 m above the bed at the base of the stoss slope, on the mid stoss slope at 0.66 m and 1.66 m, and at the crest, also at 0.66 m and 1.66 m. An additional 3-D sonic was deployed at 0.66 m height at the scarp crest. Three-dimensional velocity components (U,V and W) were measured continuously at 32 Hz for the duration of the storm event, and then subsets of 10-minute periods were extracted to characterize the range of wind velocities experienced throughout the storm event.

For the results presented here, the directional reference used in some of our previous papers at this site has been modified, such that 0° is onshore (perpendicular to the crestline of the foredune), 90° is alongshore (i.e. from the east) and 180° is offshore (i.e. winds blowing directly offshore). This was necessary for purposes of the CFD modelling. Instrument U–V planes were installed parallel to the underlying surface slope so as to limit streamline misalignment to the sensor sampling plane (Walker, 2005). No pitch corrections were applied and, therefore, mean flows in the vertical direction (i.e., perpendicular to the underlying topographic slope) imply a local streamline direction oriented either toward the surface (negative W) or away from the surface (positive W). As the sonic anemometers were installed to within +/- 1° of the slope, the time series were not adjusted for yaw, which rotates

7

the dataset to a coordinate system that is parallel to the wind streamlines. Nevertheless, the magnitude of the yaw angle for each time increment was calculated in order to provide the essential information on flow deflection.

Computational Fluid Dynamics (CFD) Methodology

Wind flow over the dune surface was simulated using CFD, which has been used successfully to simulate flow over a number of coastal dune landforms (Pattanapol et al., 2008; Wakes et al., 2010; Jackson et al., 2011; Smyth et al., 2012; 2013). Simulations in this study were performed using open-source software, OpenFOAM, which is capable of solving a range of complex fluid flows but also includes tools for meshing the surface topography and visualising the results. The wind field over the dune was simulated assuming incompressible flow using a large time-step transient solver, pimpleFoam. Turbulence was modelled using the Renormalised Group (RNG) k-epsilon method (Yakhot et al., 1992). The turbulence model is based on the Reynolds-averaged Navier-Stokes (RANS) equations, which focuses on the effects of turbulence on the average flow rather than resolving turbulence at every scale, as with direct numerical simulation (DNS) or at the larger scale like a large eddy simulation (LES). The RNG model has been used to accurately simulate near surface flow over a transverse dune in a wind tunnel (Parsons et al., 2004), coastal dune complex (Wakes et al., 2010), and a complex foredune blowout (Smyth et al., 2012; 2013). The digital elevation model used to represent the dune surface within the computational domain was generated from RTK-DGPS points collected on site prior to the experiments.

The surface of the domain was given a roughness height of 0.05 m, the same as that stated for a beach by Pattanapol et al. (2007). This height was prescribed, as at least two cells are recommended between the surface and the area of interest within the computational domain (Franke et al., 2004). In this case, the nearest field measurement point was at 0.66 m above

the surface, therefore a minimum cell height of 0.15 m was utilised. Although this is smaller than the stem height of the vegetation recorded in the field (0.3 m), the size of the near surface grid cell (0.6 m) required to include information on actual vegetation effects is too large to properly simulate the complexity of near surface flow that occurs in vegetated surfaces in the field.

A mesh independence study was completed to ensure the simulation results were independent of the mesh resolution. This was achieved by increasing the horizontal resolution of the mesh, producing an increase in the total number of cells by 40%. Results at 70 locations throughout the computational domains were compared for 2 directions and average variance in wind direction was found to be below 1% for both cases.

Flow at the upwind boundary was defined as a logarithmic profile as described by Blocken et al. (2007). The turbulence model parameters k and epsilon were given initial values of 0.325 on the assumption they would adjust to the upwind boundary conditions quickly on simulation commencement (as validated by e.g. Wakes et al., 2013, and Flores et al., 2013).

Wind flow over the dune was modelled at $10^{°}$ increments from parallel to the crest (alongshore, $90^{°}$) to perpendicular to the crest (onshore, $0^{°}$), thereby producing a total of ten flow simulations.

Modelled U, V and W components were adjusted to be slope-aligned using a clockwise rotation of the coordinate reference frame to be consistent with the field instruments. Only the modelled U and W vectors were realigned in this way since V for the field and model results were already in the same reference frame.

The U and W alignment algorithms are:

Aligned CFD U = CFD U*COSINE(slope in radians) – CFD W*SIN(slope in radians)   (1)

Aligned CFD W = CFD U*SIN(slope in radians) + W*COS(slope in radians)   (2)

Wind direction was validated graphically by comparing vectors of modelled and measured data and by percentage difference calculations (Smyth et al., 2013), as follows:

CFD wind direction % error = (measured − modelled)/360*100   (3)

CONCEPTUALIZING FLOW DEFLECTION OVER A DUNE RIDGE

Before examining the field and modelled data, it is useful to consider why flow deflection occurs when wind approaches a foredune ridge from an oblique angle. Consider an oblique, onshore coastal wind crossing a beach and encountering a linear, two-dimensional, shore-parallel dune. As noted above, field observations have shown that such an oblique wind will be subject to topographic steering effects as it progresses up the stoss slope, such that it becomes more crest-perpendicular toward the crest (e.g., Arens, 1995; Walker et al., 2006, 2009, Bauer et al., 2012). The Bernoulli equation provides a qualitative explanation for why topographic steering will occur. At the outset, however, it needs to be recognized that the Bernoulli approach presumes incompressible, irrotational flow and an inviscid fluid. As a consequence, there can be no shearing motion in the internal domain of the fluid, and therefore lateral shear forces are considered to be a secondary effect by definition. Fig. 3 shows two parallel streamlines connected by an infinitesimally small volume of air at the local ground level with mass, m, length, l, and cross-sectional area, A. The axis of the air volume along l is perpendicular to the streamlines, but forms a local angle with the dune line orientation, α. Flow velocity, V, is assumed uniform along any dune contour but is allowed to change as the streamline moves up the stoss slope as a function of streamline convergence.

Although velocity will also change with height above the bed this effect is not modelled in this two-dimensional approach.

Writing the Bernoulli Equation for the two ends of the cylindrical air volume yields,

$$P - \Delta_P + \frac{1}{2}\rho(V + \Delta_V)^2 + \rho g(Z + \Delta_Z) = P + \frac{1}{2}\rho V^2 + \rho g Z$$

$$P - \Delta_p + \frac{1}{2}\rho(V + \Delta_v)^2 + \rho g(Z + \Delta_z) = P + \frac{1}{2}\rho V^2 + \rho g Z \qquad (4)$$

where P is pressure, ρ is density, g is acceleration due to gravity, and Z is height. The standard application of the Bernoulli Equation is normally for two points along the same streamline, but when the flow is laterally uniform along a two-dimensional dune, the two streamlines through the ends of the parcel are equivalent and exchangeable. As wind moves up the dune according to the elevation difference between the two points, the near-surface flow field converges and accelerates. The flow acceleration, in turn, creates a pressure gradient, which is ultimately responsible for the steering influence.
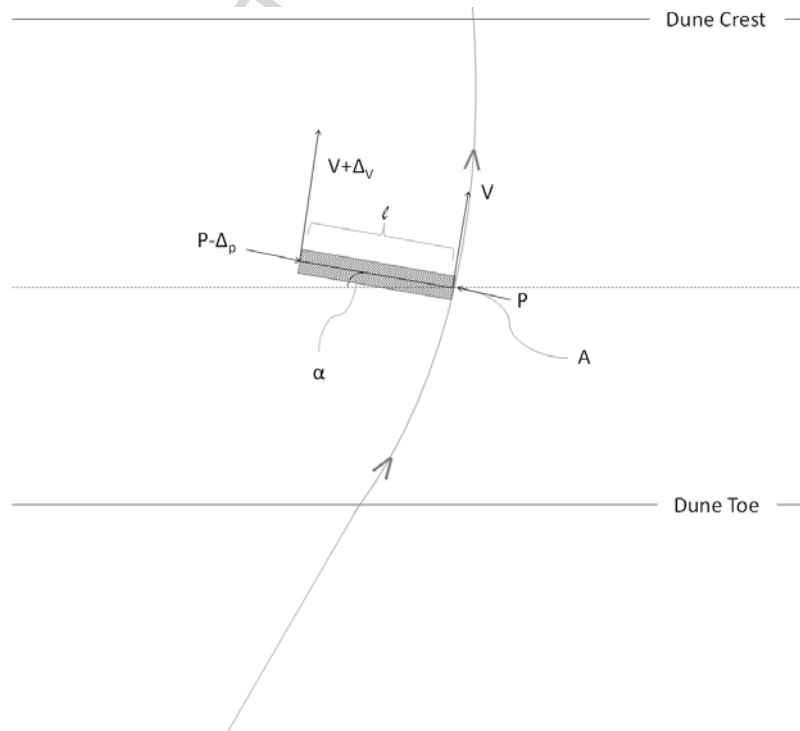
Where: l is length

A is cross section

V is velocity

α is angle normal to dune

Figure 3: Illustration of a parcel of air approaching the dune at an oblique angle. The initially oblique wind tends to become more crest-perpendicular as it climbs the dune stoss slope.

To simplify the analysis, it is useful to combine the pressure and elevation terms into a piezometric pressure $P^* = P + \rho g z$, so equation (4) becomes,

$$P^* - \Delta_{P^*} + \frac{1}{2}\rho(V + \Delta_V)^2 = P^* + \frac{1}{2}\rho V^2 \quad (5)$$

$$P^* - \Delta_{P^*} + \frac{1}{2}\rho(V + \Delta_v)^2 = P^* + \frac{1}{2}\rho V^2$$

Then, the approximate piezometric pressure difference between the ends of the air parcel can be written as (omitting a negligible term in Δ_V^2 given that the difference in velocity across the air volume is small in comparison to the absolute wind speed),

$$\Delta_{P^*} = \rho V \Delta_V \quad (6)$$

$$\Delta_{P^*} = \rho V \Delta_v$$

Svasek and Terwindt (1974; Fig. 6) implicitly followed a similar line of reasoning to reach the same conclusions.

As above, this piezometric pressure gradient Δ_{P^*} provides a net force, $F_\perp = \Delta_{P^*} A$ $F_\perp = \Delta_{P^*} A$ on the air parcel in a direction perpendicular to its trajectory, which is proportional to a rate of deflection $d\alpha/dt$ through Newton's Second Law of Motion;

$$m|V|\frac{d\alpha}{dt} = F_\perp \quad (7)$$

12

$$m|V|\frac{d\alpha}{dt} = F_\perp$$

Using the definition of the total derivative, $d/dt = V \, d/ds$, where s is the distance along a streamline, Equations 6 and 7 can be manipulated as follows,

$$m|V|\frac{d\alpha}{dt} = mV^2\frac{d\alpha}{ds} = F_\perp = -\Delta_{P*}A \approx -\rho V \Delta_V A \qquad (8).$$

$$m|V|\frac{d\alpha}{dt} = mV^2\frac{d\alpha}{ds} = F_\perp = \Delta_{P*}A \approx -\rho V \Delta_V A$$

The approximation at the end of Equation 8 is drawn from Equation 6, which ignores a small, higher order velocity gradient term. The general form of Equation 8 can be rearranged to yield,

$$\frac{d\alpha}{ds} = \frac{-\rho\Delta_V A}{mV} = -\frac{\Delta_V}{lV} \qquad (9)$$

$$\frac{d\alpha}{ds} = \frac{-\rho\Delta_V A}{mV} = -\frac{\Delta_V}{lV}$$

which shows that an increase of Δ_V / V up the dune (right hand side of equation) is balanced by an increase in the rate of deflection (left hand side of equation). Writing the velocity difference Δ_V between the two ends of the air volume in terms of the uphill acceleration dV/dz and the elevation difference $\beta l \sin \alpha$, where β is the slope of the dune surface, we arrive at a differential equation that describes the deflection of the wind (i.e., variation of α) in terms of the mean velocity, the velocity gradient in the up-dune direction, and the slope angle,

$$\frac{d\alpha}{ds} = -\frac{\beta\dfrac{dV}{dz}}{V}\sin\alpha \qquad (10)$$

13

$$\frac{d\alpha}{ds} = -\frac{\beta \frac{dV}{dz}}{V} \sin\alpha$$

Equation 10 shows that if the wind is initially perpendicular to the dune (i.e. $\sin\alpha = \alpha = 0$) there is no deflection along the streamline. If the angle of wind approach is oblique to the dune, the $\sin\alpha$ term is non-zero and wind steering occurs. The effect is most pronounced when the dune slope angle (β) is steep and the uphill acceleration (dV/dz) is strongest. Interestingly, the strength of the steering effect is inversely proportional to the mean incident wind speed, which may explain some of the variance in the empirical data regarding flow deflection over dunes. Similarly, there is a limit to this topographic forcing because with very oblique angles of wind approach, the velocity gradient becomes small as it is forced over a much longer and gentler facet of the dune (i.e., the apparent steepness or aspect ratio of the dune decreases). As a very loose approximation, $dV/dz \sim \cos\alpha$, which leads to,

$$\frac{d\alpha}{ds} \sim \sin\alpha\cos\alpha \sim \sin2\alpha \qquad (11)$$

$$\frac{d\alpha}{ds} \sim \sin\alpha\cos\alpha \sim \sin2\alpha$$

Equation 11 is zero for both 0° and 90° and maximum for $\alpha = 45^o$, corresponding to the suggestion by Svasek and Terwindt (1974) that maximum deflection should occur for $30^o < \alpha < 90^o$.

The above derivations are admittedly simplistic in as much as the Bernoulli Equation neglects friction, turbulence, flow compressibility, wind unsteadiness, and various other 3-D boundary layer dynamics that occur as the wind approach angle shifts from onshore to alongshore. Nevertheless, it provides a useful heuristic explanation of why the steering effect occurs and suggests a means to organize the empirical data into a coherent model of flow deflection that

has four controlling variables: (1) mean incident wind speed; (2) mean angle of wind approach; (3) dune slope; and (4) strength of flow acceleration up the stoss slope of the dune. Moreover, a numerical integration of (10), which can be done in a simple spreadsheet, gives reasonable wind trajectories $\alpha(s)$ based on measured V, dV/dz as long as the topography does not depart significantly from a two-dimensional form.

COMPARISON OF FIELD AND MODELLED CFD DATASETS

Fig. 4 illustrates the CFD and field data for the scarped profile during an incident wind angle of 68° measured above the beach at 4 m above the surface. The presence of the scarp exacerbates the incident flow at the toe, and tends to steer the incident flow along-scarp to some degree as observed in other studies (Svasek and Terwindt, 1974; Arens, 1995; Mikkelsen, 1989; Hesp et al., 2013). Above the scarp, the streamlines converge and the flow is accelerated (cf. Bowen and Lindley, 1977) so the velocity is greater there than farther up the stoss slope. Flow accelerates towards the crest on the upper stoss slope. At 0.66 m above the ground, the degree of flow deflection from dune toe to crest is 33°, while at 1.66 m above the ground it is 13°.

The greatest difference between the CFD results and the field data is at the dune scarp. This is to be expected as this is a highly turbulent region, the scarp tends to deflect the flow alongshore (corkscrew vortices are commonly observed here), and often turbulent jets are formed across the scarp crest (e.g. Bowen and Lindley, 1977; Hesp et al., 2009, 2013). Nevertheless, the flow deflection direction error (see Equation 3) between modelled and field data is less than 1% for five of the seven locations indicating a remarkably good agreement between the modelled and field results.

The CFD modelling also shows that there is a constant difference between the flow deflection at 0.66 m compared to 1.66 m. The near-surface wind is consistently more deflected than the upper wind, and this is also observed in the field data (cf., Walker et al., 2009).
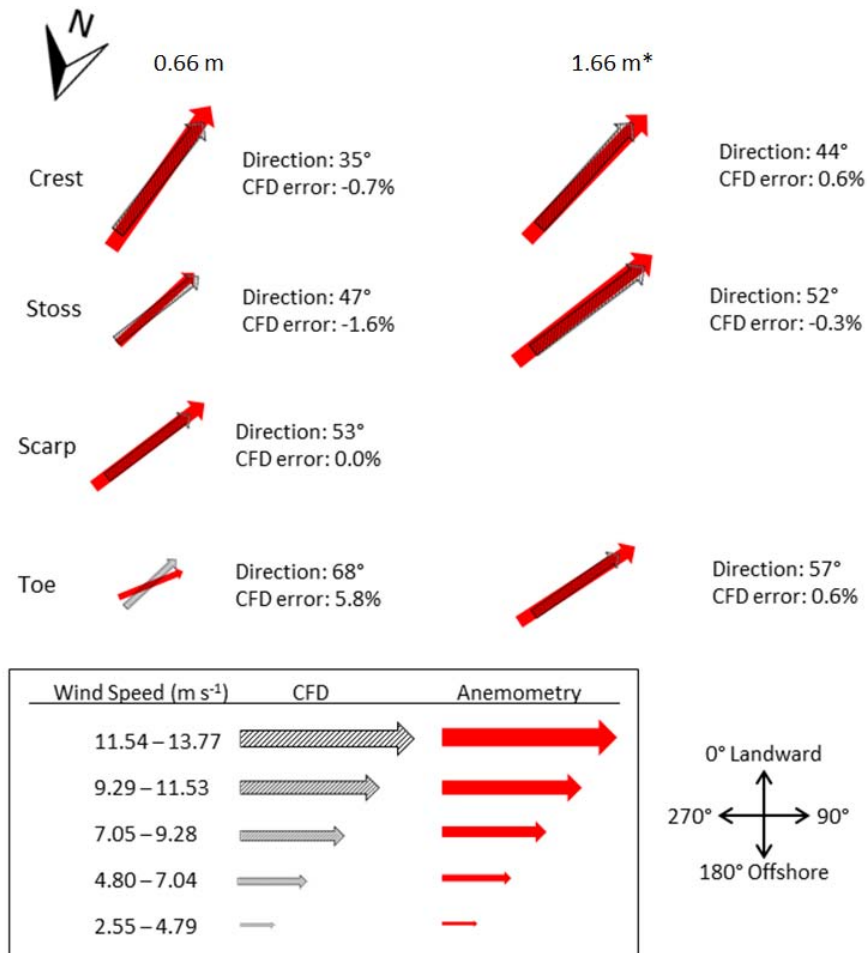

Figure 4. Comparison of field measured (in dark grey wind speed and direction and modelled (in grey) CFD results. Direction represents that recorded at each UVW anemometer. 0° is onshore perpendicular to the crest of the dune and 90° is alongshore, and 180° onshore. Note that the upper anemometer at the foredune toe is at a height of 2.05 m, while the other two are at 1.66 m height. „CFD error" in the diagram relates to wind direction only.

CFD MODELLING OF MULTIPLE INCIDENT WIND DIRECTIONS

The comparison of field and modelled data indicates that there is a good correlation between field and modelled flow deflection over the foredune. Here, we extend the range of incident winds observed in the field by modelling all onshore to alongshore winds in ten-degree increments from directly onshore ($0°$) to directly alongshore ($90°$) and examine the resulting degree of flow deflection.
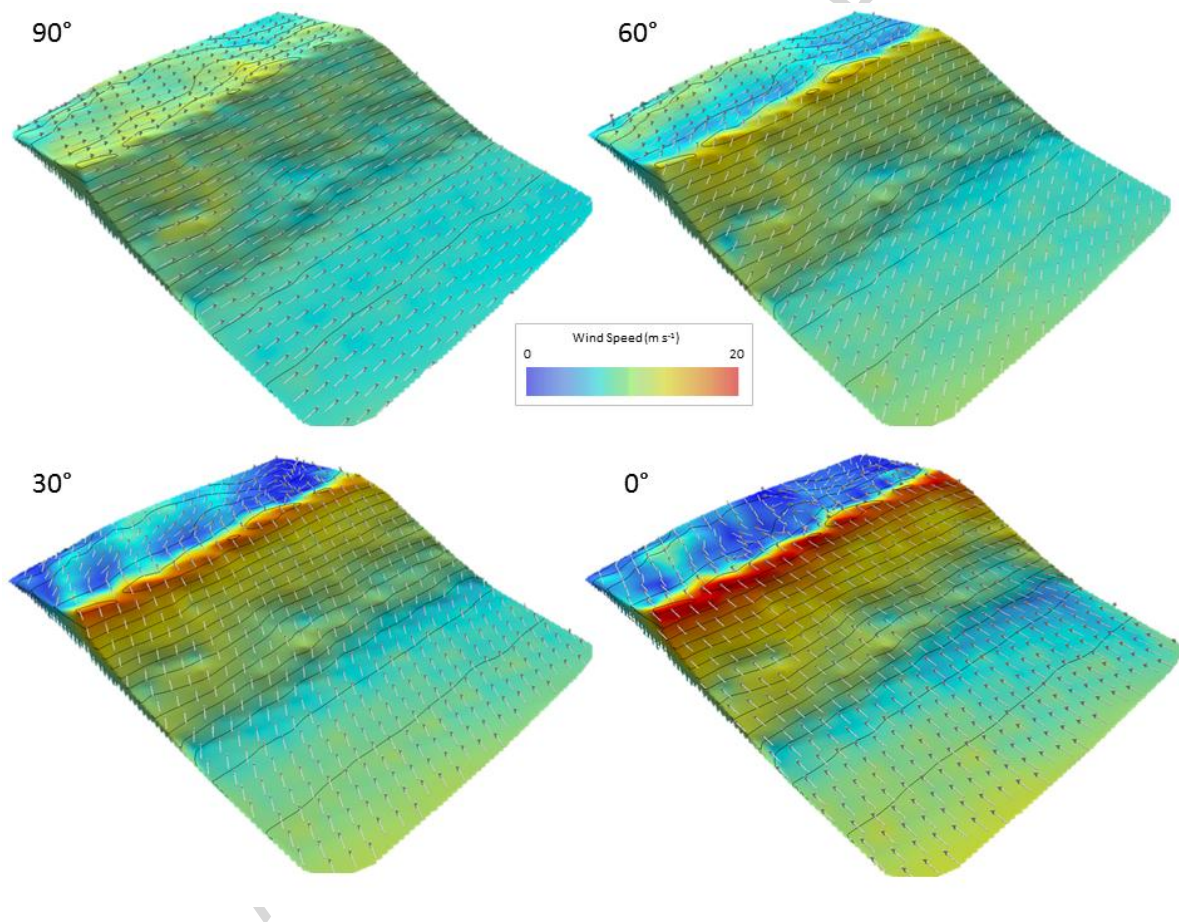

Figure 5. CFD modelled flow velocity at 0.66 m above the dune surface at 30° iterations for incident wind directions ranging from crest parallel to crest perpendicular. Arrows spaced at 2 m intervals represent wind flow direction at 0.66 m above the surface. Elevation contours are spaced at 0.5 m intervals. The incident approach speed on the beach upwind was 12.2 m s⁻

[1] at 4 m above the beach surface in all cases. The greatest topographically-forced flow acceleration and least flow deflection occurs for directly onshore winds.

Fig. 5 illustrates the 3-D flow fields produced by the CFD model for four incident wind directions at a consistent incident speed of 12.2 ms^{-1} at 4 m above the beach surface. The greatest topographically-forced flow acceleration and least flow deflection occurs for directly onshore winds. The greatest velocities occur near the foredune crest (red colours on Fig. 5). The greatest flow deflection across the dune occurs for winds in the 30° to 60° range, and the rate of deflection increases towards the dune crest (see 60° incident wind in Fig. 5). Interestingly, over this relatively uniform dune terrain, there is less lateral uniformity in the wind field when the incident wind approaches from >60° because even slight topographic variations are experienced more so by the more oblique to alongdune oriented winds.

Fig. 6 illustrates a range of incident flows at 10° increments, and shows the degree of flow deflection in 1 m increments across the foredune. When the flow is perpendicular (i.e. the zero degree lines on Fig. 6), there is minor flow deflection at both heights above the surface in the upper stoss slope region. This small degree of deflection probably results from alongshore variations in dune morphology. As the incident wind becomes more oblique, the degree of flow deflection increases to a maximum for incident winds arriving from 40° to 50°, as expected following Equation 13 and as observed by Svasek and Terwindt (1974) and Arens et al. (1995). Under those conditions, the flow is steered or deflected 20° more crest-perpendicular from the dune toe and scarp to the crest. For example, at 0.66 m above the surface and at an incident flow of 50°, the incident direction 10 m seawards of the dune scarp is approaching at ~49°. This is deflected more crest parallel to ~57° at the dune scarp, and then deflected back to ~33° and more perpendicular at the dune crest. There is consistently less flow deflection at higher elevations above the dune compared to flow nearer to the bed (Fig. 6; Table 1).

At the dune toe, the flow steers along the beach due to the presence of the scarp, and the modelling indicates significant variations in flow directions or deflections over a short distance, even for incident wind approach angle as small as 10°. This process, whereby the diverging wind flow at the dune toe which directs flow along the beach or up the stoss slope of the dune, may result in the decoupling of the dune and beach sand transport systems (Bauer et al., 2012). Note that there is often flow separation, topographic steering of flow alongshore and the common presence of corkscrew vortices in front of scarps. In addition, flow acceleration and the formation of a jet over the scarp crest commonly occurs (Bowen and Lindley, 1977; Tsoar, 1983; Hesp et al., 2009). Above and downwind of the scarp, the flow expands and becomes more crest-perpendicular as the flow crosses the stoss slope. Where the incident flow becomes more crest-parallel, there is naturally a greater tendency for the flow to steer along the scarp and the dune-parallel to the contours. Thus, there is progressively less deflection as the incident flow becomes more crest-parallel, and this is true for both anemometer heights examined.
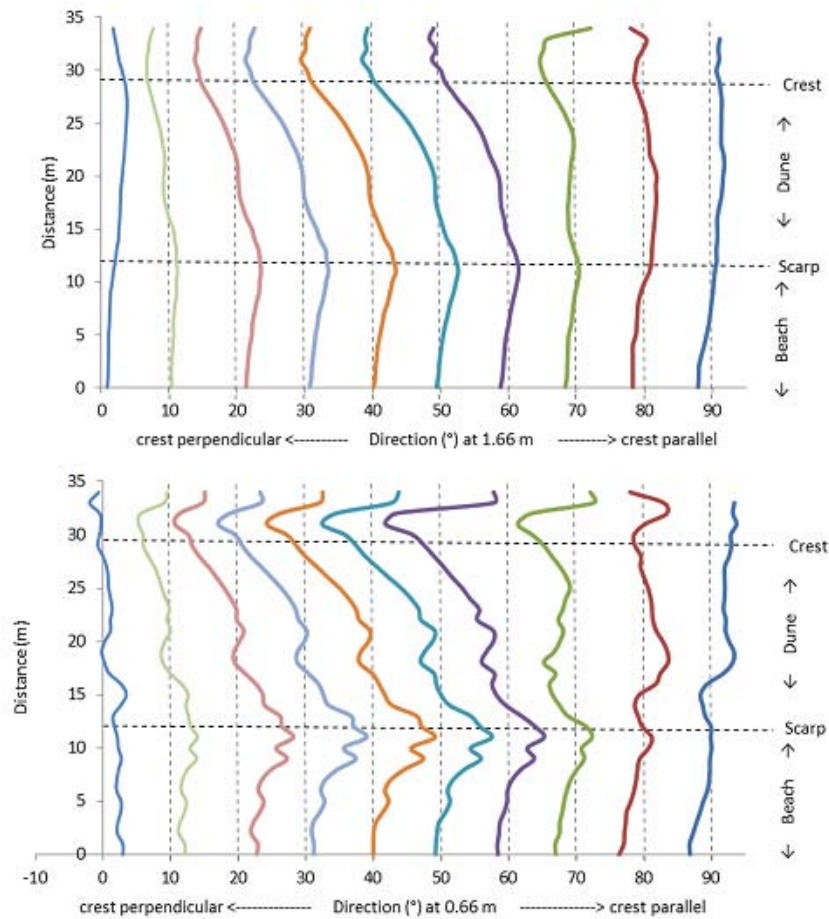
Figure 6. Direction of wind flow at 1.66 m (upper panel) and 0.66 m (lower panel) above the surface of the transect at 1 m intervals across the dune from the beach (at 0 m on the y-axis) to the dune lee slope (at ~35 m). Incident wind flow was modelled at 10° intervals from crest-perpendicular (0° and directly onshore) to crest-parallel (90° and alongshore). The greatest degree of flow deflection occurs in the 30° to 60° range.

Fig. 6 also illustrates that the flow is considerably deflected once it crosses the dune crest and into the lee-side region, more so at lower heights above the bed and as the incident wind approach angle ranges between 30° and ~60°. This is a zone where flow separation often occurs. At small angles of approach the separation flow structure is typically a simple reversing vortex (e.g., Warren, 1979; Hesp et al., 1989; Walker and Nickling, 2002; Bauer et al., 2012; Walker and Shugar, 2013), but as the incident flow increases in obliquity, the

separation zone is characterized by corkscrew vortices trending downwind (cf. Walker and Nickling 2002; Walker and Shugar, 2013). As the incident flow approaches 90° to directly along the dune crest axis, there is minimal to no flow separation and, therefore, minimal flow deflection. Again, the impact of the scarp is greater nearer to the bed compared to higher above the dune for along-dune low.

Incident wind direction	Degree difference scarp & crest	
(degrees)	0.66 m	1.66 m
90	4	0
80	1	2
70	5	5
60	16	11
50	19	12
40	19	12
30	17	11
20	14	8
10	7	4
0	2	0

Table 1. Wind direction difference (in degrees) between CFD modelled flow at the scarp base at 0.6 m high and the crest (at 1.66 m high) for the full range of incident winds (0-90°) across the western foredune transect. At 90°, for example, there is only a 4° diffference beween wind direction at the scarp and at the crest, and zero difference at 1.66 m high between the two, while at 50° incident wind there is a significant difference in flow direction between the two heights (19° versus 12°)

As noted in several studies, as wind becomes more crest-parallel, the degree of flow speed-up tends to decrease (e.g. Arens et al., 1995; Hesp, 2002; Walker et al., 2006, 2009; Bauer et al.,

2012; Hesp et al., 2013). Fig. 7 illustrates wind speeds at 1 m horizontal intervals across the dune transect for five incident wind directions. As with the previous simulations, the incident wind speed on the beach was 12.20 m s^{-1} at 4 m height. The CFD modelling shows that there is considerable directional unsteadiness and variability in the wind speed across the backshore upwind of the dune especially nearer the surface due to the positive pressure gradient induced by the dune on the flow field. It is well known that the dune toe region is an area of considerable deceleration or speed-down (cf. Bowen and Lindley, 1977) and flow unsteadiness as turbulent flow structures are conveyed toward the bed in an area of rapid slope change (e.g., Wiggs et al., 1996, Walker and Nickling 2002, Walker et al., 2006, Chapman et al., 2012), and this is also more pronounced at or near the lower stoss slope. From the mid-stoss slope to the crest, the greatest flow acceleration occurs for perpendicular to low obliquity winds (10-30$^{°}$) and uniformly decreases as the incident wind direction swings to 50$^{°}$, at both heights (0.66 and 1.66 m) above the surface.

There is flow separation at, and beyond, the foredune crest as visualized by multiple videos taken in the field of smoke bomb flow patterns (e.g. Walker, 2005; Fig. 6) for perpendicular and low to moderate obliquity winds. The flow structure is typically a simple reversing roller vortex in this region (Bauer et al., 2012) and this flow separation zone drives significant deceleration in wind speeds leeward of the dune crest as in Fig. 7. As the flow trends towards more crest parallel (from 50$^{°}$ towards 70$^{°}$), the degree of flow deceleration declines leeward of the crest at 0.66 m above the bed and this pattern holds for winds higher above the surface (1.66 m). In effect, the dune profile or topography that the 70$^{°}$ incident wind encounters is still relatively steep and asymmetric. Once the incident wind approaches from 90° to crest parallel, there is typically significantly less to no flow separation across the dune crest and extending on the lee slope, so the isovel distribution is quite different compared to other incident flows. Overall, the CFD modelling demonstrates that the degree of topographically

accelerated flow decreases as the incident wind becomes increasingly more oblique to the foredune. At 0.66 m above the bed, for example, the wind speed at the foredune crest for an incident wind direction of $50°$ and $80°$ is on average 25% lower than for winds in the 0 to $30°$ incident range. As found in a much simpler CFD simulation by Parsons et al. (2004), however, dune height is perhaps more important than aspect ratio (h/L) in controlling near-surface flow response over dunes, particularly at the crest. This is because total vertical displacement of flow streamlines and resulting flow acceleration responses are fundamentally greater over taller dunes. Although the flow responses observed here are a function of the observed dune geometry (i.e., a 10 m tall foredune), this study provides a more comprehensive picture of flow deflection and acceleration behaviour over foredunes in response to the full range of onshore incident flow angles.
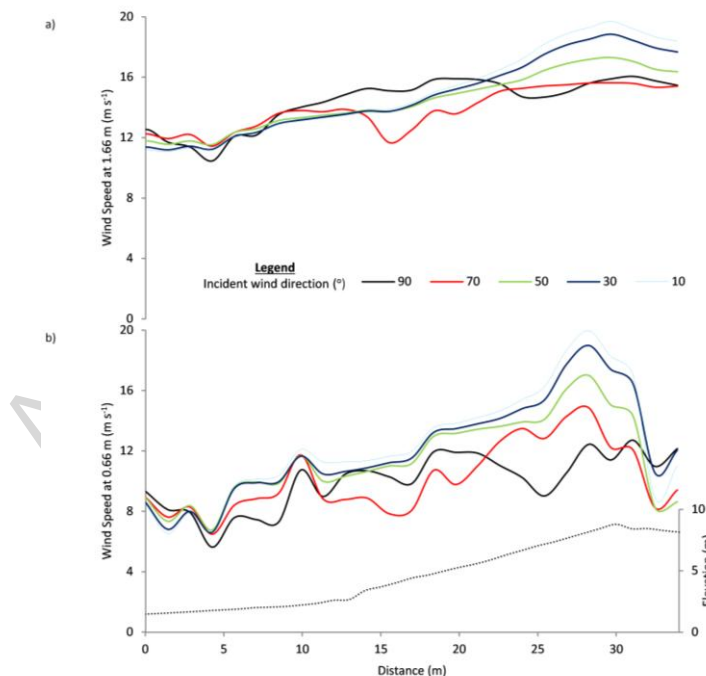

Figure 7. (a) Wind speed at 1.66 m above the dune at 1 m intervals for five incident wind directions. (b) Wind speed at 0.66 m above the dune at 1 m intervals. The greatest speed-up

occurs for winds that are most perpendicular and, therefore, where the topography is steepest and then decreases as the incident wind becomes increasingly oblique up to ~70°.

Fig. 8 summarises the general flow conditions and degree of deflection that occurs in the 0 to 3 m boundary layer above the beach and foredune. It illustrates three examples of incident flow approaching the dune from 20°, 40° and 80°. At 20° there is slight decoupling and deflection to the right near the scarp and then deflection towards more crest-normal on the mid to upper stoss slope. At 40°, the extent of deflection is considerable and there is greater deflection of the lowermost streamlines compared to the upper ones. In both the 20° and 40° examples, the velocity is greatest near the crest (indicated by the red colours). At 80° there is significantly less overall deflection of the streamlines compared to that at 20° and 40°, but some still occurs. Speed-up is considerably less than in the 20° and 40° cases, and local velocity variations are primarily due to changes in surface morphology.
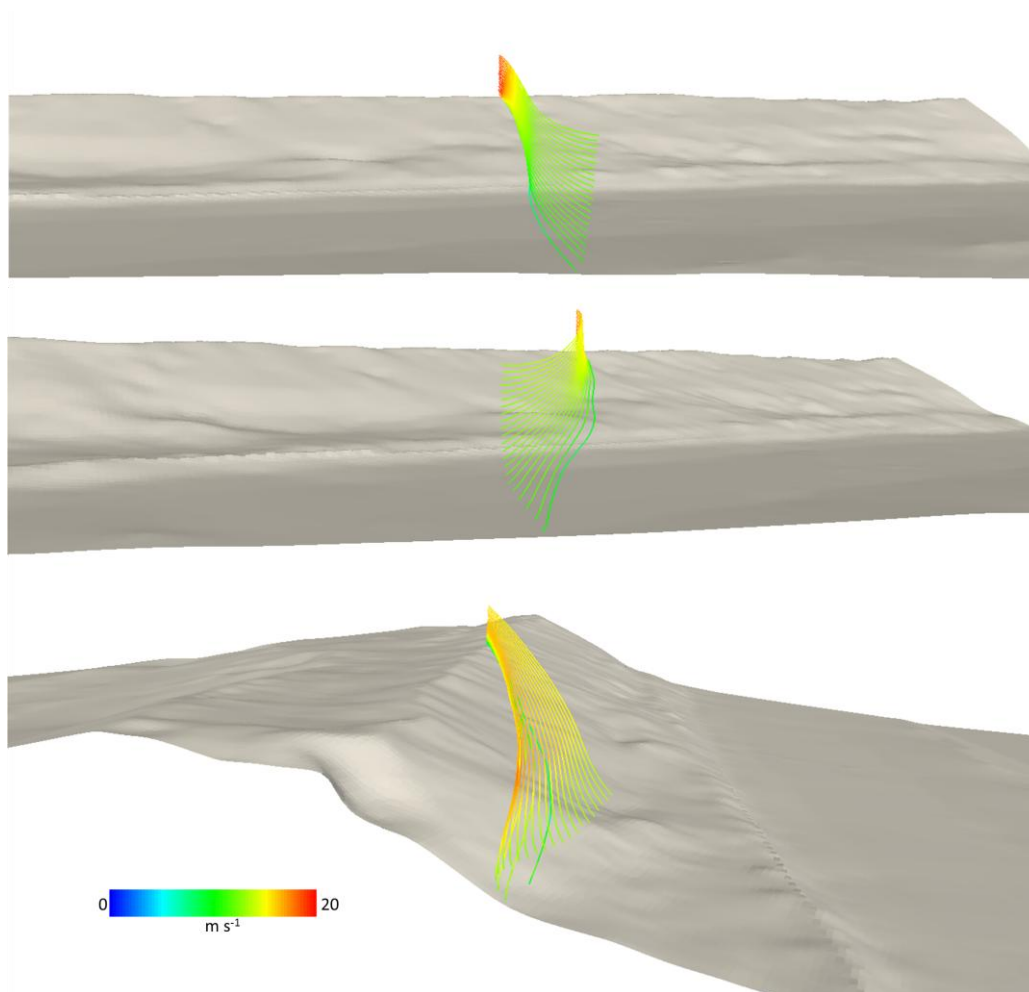
Figure 8: Examples of lower boundary layer flow (0.66 to 2 m range) and degree of streamline deflection for three incident wind approach directions, 20° (uppermost), 40° (middle) and 80° (lowermost). The lowest streamlines show the strongest response to variations in surface morphological changes and display the greatest degree of deflection.

CONCLUSIONS

A comparison of field data collected during oblique winds and CFD modelling demonstrates that the CFD simulations are able to provide good agreement with field data. This allows for simulation of a complete range of incident flows from onshore to alongshore (0-90°) and interpretation of near-surface flow deflection and acceleration patterns. This study provides

25

the first examination of such flow dynamics over a foredune ridge and provides several new insights. Key findings, include:

(i)   deflection of the incident wind flow is minimal at $0°$ although minor deflection occurs because the foredune is never perfectly smooth and „prismatic";

(ii)   deflection gradually increases as the incident wind turns towards $30°$ to the dune;

(iii)   the greatest degree of flow deflection occurs in the $30°$ to $70°$ range, and is maximum at $\sim45°$ as it is proportional to $\sin 2\alpha$;

(iv)   there is a consistent difference in the degree of flow deflection with height above the dune, with the greatest steering occurring closest to the surface confirming observations in previous field studies;

(v)   the degree of deflection increases towards the dune crest;

(vi)   speed-up or topographically-forced flow acceleration up the foredune is strongly affected by the incident wind flow approach direction, such that speed-up is greatest for perpendicular to $30°$ oblique incident winds and declines significantly for winds $>30°$ as the speed-up is proportional to $\cos\alpha$

(vii)   there is less lateral uniformity in the wind field when the incident wind approaches from $>60°$ because the greater along-dune (compared to across-dune) topographic variations are "seen" more by the higher angle oblique to along-dune winds;

(viii) in the lee zone, large variations in flow deflection occur because of potential flow separation at the crest. Differences in the degree of deflection at $\sim70°$ incident wind flow may be due to the onset of corkscrew vortex generation compared to relatively stationary roller vortices at perpendicular to $<50°$ incident winds.

Deflection of oblique incident winds across a foredune has important implications for foredune evolution, sedimentation, stratification and palaeoenvironmental interpretations.

26

For coastal environments where the winds are predominantly oblique to the coastline, across-dune sand transport pathways will be more shore-transverse than predicted from regional wind analyses, sedimentation patterns will mimic that trend, and the subsequent stratification patterns, stratal dips and cross-bed azimuths will be more variable across the dune from toe to crest than anticipated or modelled.

ACKNOWLEDGEMENTS

References

Arens, S.M., 1996. Patterns of sand transport on vegetated foredunes. Geomorphology 17: 339-350.

Arens, S.M., van Kaam-Peters, H.M.E., van Boxel, J.H., 1995. Air flow over foredunes and implications for sand transport. Earth Surface Processes and Landforms 20: 315-332.

Ayotte, K.W., Hughes, D.E., 2004. Observations of boundary-layer wind-tunnel flow over isolated ridges of varying steepness and roughness. Boundary-Layer Meteorology 112: 525-556.

Baddock, M. C., Livingstone, I., & Wiggs, G. F. S. (2007). The geomorphological significance of airflow patterns in transverse dune interdunes. Geomorphology, 87(4): 322-336. doi:10.1016/j.geomorph.2006.10.006

Bauer, B.O., Davidson-Arnott, R.G.D., Walker, I.J., Hesp, P.A., Ollerhead, J., 2012. Wind direction and complex sediment transport response across a beach-dune system. Earth Surface Processes and Landforms 37 (15): 1661-1677.

Bauer, B.O., Davidson-Arnott, R.G.D., Hesp, P.A., Namikas, S.L., Ollerhead, J., Walker, I.J., 2009. Aeolian sediment transport conditions on a beach: Surface moisture and wind fetch effects on mean transport rates. Geomorphology 105 (1-2): 106-116.

Bauer, B.O., Walker, I.J., Baas, A.C.W., Jackson, D.W.T., Mckenna Neuman, C., Wiggs, G.S.F., Hesp, P.A., 2013, Critical Reflections on the Coherent Flow Structures Paradigm in Aeolian Geomorphology. In: J.G. Venditti, J.L. Best, M. Church, and R.J. Hardy (eds.), Coherent Flow Structures at the Earth's Surface. Wiley-Blackwell: 111-134.

Belcher, S.E., Hunt, J.C.R., 1998. Turbulent flow over hills and waves. Annual Review of Fluid Mechanics 30: 507-538.

Blocken, B., Stathopoulos, T., Carmeliet, J., 2007. CFD simulation of the atmospheric boundary layer : wall function problems, Atmospheric Environment 41: 238–252.

Bowen, A.J., Lindley, D., 1977. A wind-tunnel investigation of the wind speed and turbulence characteristics close to the ground over various escarpment shapes. Boundary-layer Meteorology 12: 259-271.

Bradley, E.F., 1983.the influence of thermal stability and angle of incidence on the acceleration of wind up a slope. J. Wind Engineering and Industrial Aerodynamics 15: 231-242.

Chapman, C.A., Walker, I.J., Hesp, P.A., Bauer, B.O., Davidson-Arnott, R.G., 2012. Turbulent Reynolds stress and quadrant event activity in wind flow over a coastal foredune. Geomorphology 151-152: 1-12.

Chapman, C.A., Walker, I.J., Hesp, P.A., Bauer, B.O., Davidson-Arnott, R.G., Ollerhead, J., 2013. Reynolds stress and sand transport over a foredune. Earth Surface Processes and Landforms 38 (14): 1735-1747.

Davidson-Arnott, R.G.D., Yanqi Yang, Ollerhead, J., Hesp, P.A., Walker, I.J., 2008. The effects of surface moisture on aeolian sediment transport threshold and mass flux on a beach. Earth Surface Processes and Landforms 33: 55-74.

Davidson-Arnott, R.G.D., Bauer, B.O., Walker, I.J., Hesp, P.A., Ollerhead, J., Delgado-Fernandez, I., 2009. Instantaneous and mean aeolian sediment transport rate on beaches: an intercomparison of measurements from two sensor types. J. Coastal Research SI 56: 297-301.

Davidson-Arnott, R.G.D., Bauer, B.O., Walker, I.J., Hesp, P.A., Ollerhead, J., Chapman, C., 2012. High-frequency sediment transport responses on a vegetated foredune. Earth Surface Processes and Landforms 37 (11): 1227-1241, doi:10.1002/esp.3275

Delgado-Fernandez, I., Davidson-Arnott, R. G., and Ollerhead, J., 2009. Application of a remote sensing technique to the study of coastal dunes. Journal of Coastal Research: 25 (5): 1160-1167.

Delgado-Fernandez, I., Davidson-Arnott, R.D.A., Bauer, B.O., Walker, I.J. and Ollerhead, J., 2013. Evaluation of the optimal resolution for characterizing the effect of beach surface moisture derived from remote sensing on Aeolian transport and deposition. *In:* Conley, D.C., Masselink, G., Russell, P.E. and O'Hare, T.J. (eds.), Proceedings 12th International Coastal Symposium (Plymouth, England), Journal of Coastal Research, Special Issue No. 65: 1277-1282.

Finnigan, J.J., Raupach, M.R., Bradley, E.F., Aldis, G.K., 1990. A wind tunnel study of turbulent flow over a two-dimensional ridge. Boundary-Layer Meteorology 50 (Issue 1-4):277-317.

Franke, J., Hirsch, C., Jensen, A.G., Kru¨ s, H.W., Schatzmann, M., Westbury, P.S., Miles, S.D., Wisse, J.A., Wright, N.G., 2004. Recommendations on the use of CFD in wind engineering. In: van Beeck, J.P.A.J. (Ed.), COST Action C14, Impact of Wind and Storm on City Life Built Environment. Proceedings of the International Conference on Urban Wind Engineering and Building Aerodynamics, 5–7 May 2004. von Karman Institute, Sint-Genesius-Rode, Belgium.

Hesp, P.A., 2002. Foredunes and Blowouts: initiation, geomorphology and dynamics. Geomorphology 48: 245-268.

Hesp, P.A., Illenberger, W., Rust, I., McLachlan, A., Hyde, R., 1989. Some aspects of transgressive dunefield and transverse dune geomorphology and dynamics, south coast, South Africa. Zeitschrift fur Geomorph. Suppl-Bd 73: 111-123.

Hesp, P.A., Walker, I.J., 2012. Three-dimensional æolian dynamics within a bowl blowout during offshore winds: Greenwich dunes, Prince Edward Island, Canada. Aeolian Research 3: 389-399.

Hesp, P.A., Walker, I.J., Davidson-Arnott, R.G., Ollerhead, J., 2005. Flow dynamics over a vegetated foredune at Prince Edward Island, Canada. Geomorphology 65: 71-84.

Hesp, P.A., Walker, I.J., Namikas, S.L., Davidson-Arnott, R.G., Bauer, B.O., Ollerhead, J., 2009. Storm wind flow over a foredune, Prince Edward Island, Canada. J. Coastal Research SI 56: 312-316.

Hesp, P.A., Walker, I.J., Chapman, C., Davidson-Arnott, R.G., and Bauer, B.O., 2013. Æolian dynamics over a foredune, Prince Edward Island, Canada. Earth Surface Processes and Landforms 38 (1): 1566-1575.

Jackson, D.W. T., Beyers' J.H.M., Lynch' K., Cooper' J.A.G., Baas' A.C.W., Delgado-Fernandez, I, 2011. Investigation of three-dimensional wind flow behaviour over coastal dune morphology under offshore winds using computational fluid dynamics (CFD) and ultrasonic anemometry Earth Surface Processes and landforms 36 (8): 1113-1124.

Jackson, P.S., 1977. Aspects of surface wind behaviour. Wind Engineering 1: 1-14.

Jackson, P.S., 1979. The influence of local terrane features on the site selection for wind energy generating systems. Report BLWT-1-1979, Faculty of Engineering Science, The University of Western Ontario, London, Ontario, Canada.

Lynch, K., Jackson, D.W.T., Cooper, J.A.G., 2008. Aeolian fetch distance and secondary airflow effects: the influence of micro-scale variables on meso-scale foredune development. ESPL 33: 991-1005.

Lynch, K., Jackson, D.W.T., Cooper, J.A.G., 2009. Foredune accretion during offshore winds. Geomorphology 105:139-146.

Lynch, K., Delgado-Fernandez, I., Jackson, D.W.T., Cooper, J.A.G., Baas, A.C.W., Beyers, J.H.M., 2013. Alongshore variation of aeolian sediment transport on a beach, under offshore winds. Aeolian Research 8: 11-18.

Mikklesen, H.E., 1987. Wind flow and sediment transport over a low coastal dune. Geoskrifter nr. 32. Institute of Geology, University of Aarhus, Denmark. 60pp.

Ollerhead,J., Davidson-Arnott, R., Walker, I.J., Mathew, S., 2013. Annual to decadal morphodynamics of the foredune system at Greenwich Dunes, Prince Edward Island, Canada. Earth Surface Processes and Landforms 38 (3): 284–298.

Parsons, D.R., Walker, I.J., Wiggs, G.F.S., 2004. Numerical modelling of flow structures over idealized transverse aeolian dunes of varying geometry. Geomorphology 59: 149–164.

Pattanapol, W., Wakes, S.J., Hilton, M.J., Dickinson, K.J.M., 2007. Modeling of Surface Roughness for Flow Over a Complex Vegetated Surface. Engineering and Technology 26: 271-281.

Rasmussen, K.R., 1989. Some aspects of flow over coastal dunes. Proc Royal Soc. Edinburgh 96B: 129-147.

Rubin, D.M., Rubin, A.M., 2013. Origin and lateral migration of linear dunes in the Qaidam Basin of NW China revealed by dune sediments, internal structures, and optically stilulated

luminescence ages, with implications for linear dunes on Titan: discussion. GSA Bulletin 125: 1943-1946.

Smyth, T.A.G., Jackson, D.W.T., Cooper, J.A.G., 2011. Computational fluid dynamic modelling of three-dimensional airflow over dune blowouts. Journal of Coastal Research, 64: 314-318 .

Smyth, T.A.G., Jackson, D.W.T., Cooper, J.A.G., 2012. High resolution measured and modelled three-dimensional airflow over a coastal bowl blowout. Geomorphology 177-178: 62-73.

Smyth, T.A.G., Jackson, D.W.T., Cooper, J.A.G., 2013. Three dimensional airflow patterns within a coastal blowout during fresh breeze to hurricane force winds. Aeolian Research, 9: 111-123.

Smyth, T.A.G., Jackson, D.W.T., Cooper, J.A.G., 2014. Airflow and aeolian sediment transport patterns within a coastal trough blowout during lateral wind conditions, Earth Surface Processes and Landforms 39 (14): 1847-1854.

Svasek, J.N., Terwindt, J.H.T., 1974. Measurements of sand transport by wind on a natural beach. Sedimentology 21: 311-322.

Tsoar, H., 1983a. Dynamic processes acting on a longitudinal (seif) sand dune. Sedimentology 30: 567-578.

Tsoar, H., 1983b. Deflection of sand movement on a sinuous longitudinal (seif) dune. Sedimentary Geology 36: 25-39.

Wakes, S.J., Maegli, T., Dickinson, K.J., Hilton, M.J., 2010. Numerical modelling of wind flow over a complex topography. Environmental Modelling & Software 25, 237-247.

Wakes, S., 2013. Three-dimensional Computational Fluid Dynamic experiments over a complex dune topography 1337-1342.

Walker, I.J., 1999. Secondary airflow and sediment transport in the lee of a reversing dune. Earth Surface Processes and Landforms 24 (5): 437-448.

Walker, I.J., 2005. Physical and logistical considerations of using ultrasonic anemometers in aeolian sediment transport research. Geomorphology 68: 57-76.

Walker, I.J., Hesp, P.A., R. Davidson-Arnott, R.G., Ollerhead, J., 2006. Topographic steering of alongshore flow over a vegetated foredune: Greenwich dunes, Prince Edward Island, Canada. J. Coastal Research 22 (5): 1278-1291.

Walker, I.J., Davidson-Arnott, R.G.D., Hesp, P.A., Bauer, B.O., Ollerhead, J., 2009. Mean flow and turbulence responses in airflow over foredunes: new insights from recent research. J. Coastal Research SI 56: 366-370.

Walker, I.J., Hesp, P.A., Davidson-Arnott, R.G.D., Bauer, B.O.,Namikas, S.L., Ollerhead, J., 2009. Responses of 3-D flow to variations in the angle of incident wind and profile form of dunes: Greenwich Dunes, Prince Edward Island, Canada. Geomorphology 105 (1-2): 127-138.

Walker I.J., Nickling, W.G. 2002. Dynamics of secondary airflow and sediment transport over and in the lee of transverse dunes. Progress in Physical Geography 26: 47-75.

Walker, I. J., & Shugar, D. H. (2013). Secondary flow deflection in the lee of transverse dunes with implications for dune morphodynamics and migration. Earth Surface Processes and Landforms, 38(14): 1642-1654. doi:10.1002/esp.3398

Warren, A., 1979. Aeolian processes. In: Embleton, C., Thornes, J. (Eds.), Process in Geomorphology. Edward Arnold: 325-351

Weng, W.S., Hunt, J.C.R., Carruthers, D.J., Warren, A., Wiggs, G.F.S., 1991. Air flow

and sand transport over sand dunes. Acta Mechanica [Suppl] 2: 1-22

Wiggs, G. F., Livingstone, I., Warren, A., 1996. The role of streamline curvature in sand

dune dynamics: evidence from field and wind tunnel

measurements. Geomorphology, 17(1): 29-46.

Wood, N., 2000. Wind flow over complex terrain: a historical perspective and the

prospect for large-eddy modelling. Boundary-layer Meteorology 96: 11-32.

Graphical abstract
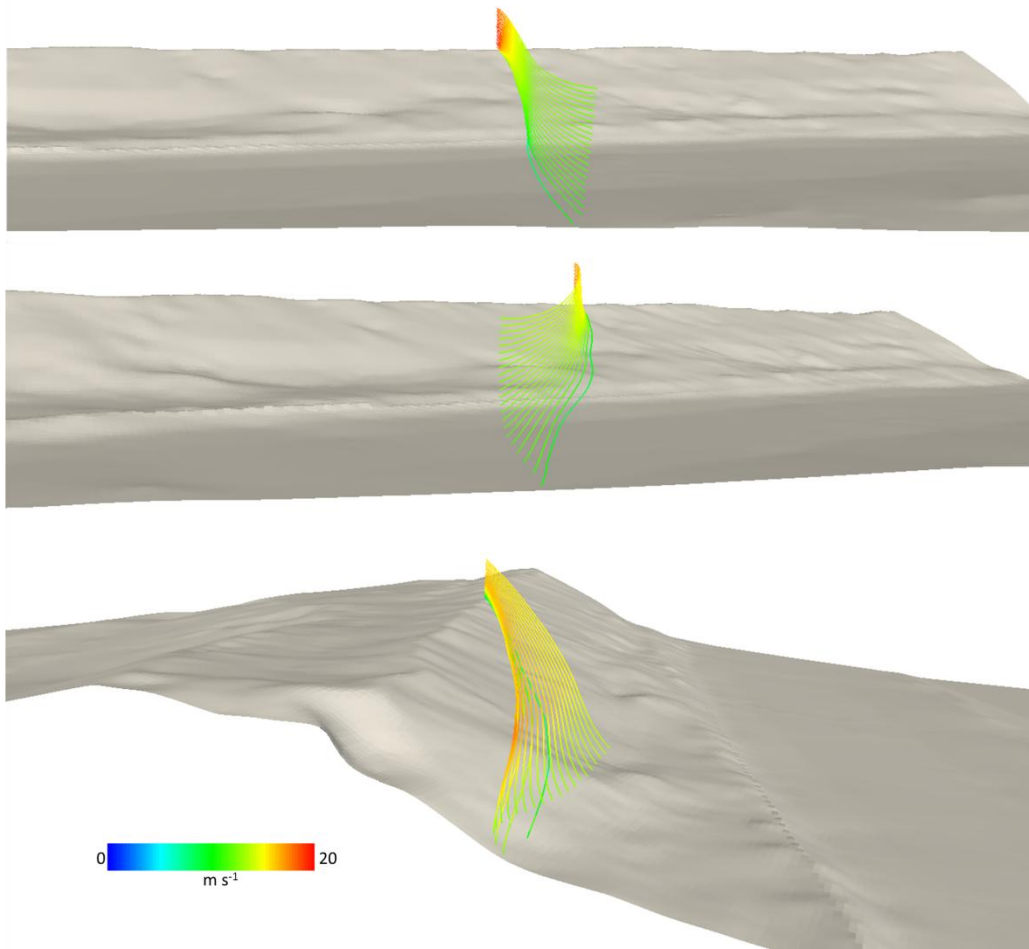
HIGHLIGHTS

- Field measurements for oblique winds over a foredune are compared to CFD modelling of flow deflection.
- The mechanics of flow deflection are outlined.
- Deflection of the incident wind flow is minimal at $0°$ and greatest at ~$45°$.
- Deflection decreases with height above the surface.
- Topographically-forced flow acceleration across the stoss slope is greatest for winds less than $30°$.